Raman scattering study of the triangular-lattice antiferromagnet VCl_2

1993 J. Phys.: Condens. Matter 5 1427

(http://iopscience.iop.org/0953-8984/5/9/027)

J. Phys.: Condens. Matter 5 (1993) 1427–1436. Printed in the UK

Raman scattering study of the triangular-lattice antiferromagnet VCl_2

K Sugawara and I Yamada

Department of Physics, Faculty of Science, Chiba University, Yayoi-cho, Inage-ku, Chiba 263, Japan

Received 16 October 1992

Abstract. We report the experimental results of a Raman scattering study of magnons in the layered triangular-lattice Heisenberg antiferromagnet VCl_2. The magnetic phase transition of this compound is said to reflect the mechanism of the dissociation of the Z_2 vortex proposed by Kawamura and Miyashita (KM). As well as two phonon lines, which agree with a group theoretical analysis, three lines are detected at low temperatures; however, they disappear around $T_N = 36$ K. Two lines among these three are attributed to the two-magnon process on the assumption that the Néel state forms a three-sublattice structure, i.e. a 120° spin structure in the ac plane. The rapid decrease of their intensity above T_N is unusual; this phenomenon, we believe, should be understood on the basis of the generation of Z_2 vortices. However, the origin of the other line is hard to explain using conventional spin-wave theory.

1. Introduction

Magnetic compounds with a hexagonal layered structure have been widely studied by various experimental methods. The representative examples are MBr_2 and MCl_2 (where M = Mn, Fe, Co, Ni) which have CdI_2 and $CdCl_2$ lamellar structures, respectively. Owing to their layered structure the magnetic two-dimensionality is excellent, but not as good as the K_2MF_4-type compounds. Although they show their individual characteristic magnetic properties, the spins order collinearly in all of them. Thus no phenomena that are against the Néel state are found. Recently, Kadowaki and co-workers [1, 2] paid attention to VCl_2 and VBr_2, which also have a CdI_2-type structure, and made thorough experimental studies on them. Their motivation was to examine the effect of full competition of the exchange interactions expected in a two-dimensional Heisenberg antiferromagnet on a triangular lattice, and it was for this purpose that they used $VCl_2$and VBr_2. They expected that magnetic phenomena arising from such an effect would not be explicable using the conventional theory of antiferromagnets.

The background to their motivation is as follows. Two decades ago, Anderson [3] pointed out that the ground state of a triangular-lattice Heisenberg antiferromagnet with $S = \frac{1}{2}$ is completely different from the Néel state for classical spin systems. As well as quantum effects, it is known theoretically that no phase transition occurs at non-zero temperatures in the two-dimensional triangular-lattice antiferromagnets

0953-8984/93/091427+10$07.50

with an exchange interaction of the Heisenberg or XY type, even if their spins are classical. In this respect, experimental studies of such magnetic systems have been anticipated.

The compounds VCl_2 and VBr_2 were expected to be suitable for an examination of the theories mentioned above, though their spin value is $S = \frac{3}{2}$ and they have been investigated intensively by measurements of susceptibility [4], neutron diffraction [1, 2], ESR [5], magnetic specific heat [6], and so on. The susceptibility of these two compounds, obtained by Niel and co-workers [7] before this series of studies, shows no phase transition, which gave an impression of the possibility of the new type of phenomenon introduced above. In spite of this expectation, the magnetic-ordered state of VCl_2 and VBr_2 was found to realize the Néel state, probably forming a three-sublattice structure, i.e. the spins make an angle of 120° with one another in the ac plane. However, several experimental results are hard to understand on the basis of conventional theories of antiferromagnets.

As studies on VCl_2 and VBr_2 have progressed [1, 2, 4–6], it has become clear that a theory proposed by Kawamura and Miyashita (KM) [8] is realized in these magnets. Kawamura and Miyashita suggested that a Heisenberg antiferromagnet on a triangular lattice undergoes a peculiar phase transition at a temperature given by $T_{KM} = 0.66|J|S^2$. They found, from a homotopy group analysis, that there is a vortex, called the Z_2 vortex, in a two-dimensional Heisenberg antiferromagnet on a triangular lattice. According to their theory, the Z_2 vortex is a topologically stable point defect formed by chiral vectors, and the phase transition at T_{KM} is caused by the dissociation of the Z_2 vortices. However, no measurable quantity diverges at T_{KM} because the spin correlation decays exponentially, even in the low-temperature phase.

As mentioned above, neutron diffraction and other studies revealed that VCl_2 and VBr_2 turn into 3D-ordered states below 36 K and 29 K, respectively, probably due to the non-negligible interlayer exchange interaction; thus no phenomenon suggested by KM was observed below T_N. The critical indices, however, agree well with the values of the KM theory. As well as these two compounds, it was pointed out that $LiCrO_2$ and $HCrO_2$, both having a layered structure, exhibit the effect of the Z_2 vortex in their EPR linewidth [9].

Prior to the above-mentioned series of reports [1, 2, 4–6], Bauhofer and co-workers [10] reported the experimental results of Raman scattering made on VX_2 (where X = Cl, Br and I). In contrast to VCl_2 and VBr_2, VI_2 was known to show an additional magnetic phase transition at ~ 13 K, from a 120° structure to a collinear arrangement, as well as the one at $T_N = 16$ K [11]. They succeeded in explaining the magnetic Raman signals of VI_2 observed below 13 K in an elegant way. They attributed those lines to inelastic scattering from zone-boundary phonons, which become Raman active due to zone-folding effects induced by elastic magnetic scattering from the antiferromagnetic spin superstructure. The spin-dependent electron–phonon coupling was identified as a modulation of the exchange interactions by selected zone-boundary phonons: $\mathcal{H}_{ep} \propto \xi \sum (1/r_{ij})(\partial J_{ij}/\partial r_{ij}) \sum_{i>j} r_{ij} S_i \cdot S_j$, where ξ is the phonon polarization vector. According to their analysis, $\sum r_{ij} S_i \cdot S_j$ yields a non-zero value in a triangular antiferromagnet with the collinear spin structure of VI_2 at low temperature, and results in the Raman signals.

However, no adequate explanation was given in [10] for the compounds VCl_2 and VBr_2, because at that time there was no clear evidence for a magnetic ordering in these compounds; the collinear magnetic structure of VI_2 [11] was known, but only

the susceptibility data obtained by Niel and co-workers [7] was available for VCl_2 and VBr_2.

Taking into account these theoretical and experimental results, we performed a Raman scattering experiment on VCl_2 in order to investigate how the magnetic signal arising from spin excitation appears in the Raman spectra, and whether or not they can be interpreted on the basis of conventional spin-wave theory. Since the magnetic properties of VCl_2 and VBr_2 reported so far are almost identical, we focused our attention on VCl_2.

2. Crystallographic and magnetic properties of VCl_2

The compound VCl_2 has a CdI_2-type hexagonal structure, with two hexagonal layers of V^{2+} ions separated by two layers of Cl^- ions, and is assigned to the space group D^3_{3d}. The crystal structure is shown in figure 1. We find that the V sites are located on a triangular lattice. No crystallographic transition is reported below room temperature. We take x, y and z to be the laboratory axes, with z parallel to the c axis, as shown in figure 1.

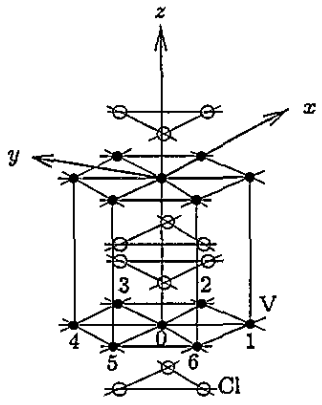

Figure 1. Crystal structure of VCl_2. The laboratory axes x, y and z are shown. The numbers 0–6 indicate the spin sites that are used in the calculation of the spin-dependent electric polarizability.

The magnetic parameters of VCl_2 determined so far are as follows. Clear three-dimensional ordering was found at 36 K [1, 2, 5, 6]. Owing to its layered structure, the intralayer exchange interaction, J, is far larger than that of the interlayer interaction, J', i.e. $J = 22$ K and $J' = 0.135$ K [1]; both interactions are antiferromagnetic. The single-ion anisotropy $D\sum_i (S_i^z)^2$ is very weak, as the value $|D| \simeq 0.05 \sim 0.09\,\mathrm{cm}^{-1}$, estimated from the g values $g_a = 1.974$ and $g_c = 1.970$ [5], indicates.

3. Experimental procedure and results

High-quality single crystals of VCl_2 were offered to us by Professor Hirakawa. They were dark green in colour. Because the surfaces exfoliated easily, we could not polish

their surfaces. Moreover, air or moisture easily acted upon them, and turned V^{2+} into V^{3+}. Therefore, in order to get flat planes, we cleaved and cut the crystals in a dry nitrogen box. Although the planes perpendicular to the c axis were obtained using this procedure, the surfaces were finely ridged. Furthermore, it was impossible to get flat planes parallel to the c axis because of their fragility. A sample of size $5 \times 4 \times 1\,mm^3$ was carefully inserted into a liquid helium cryostat; we kept the sample in a nitrogen atmosphere when removing it from the dry box to the cryostat. To obtain low temperatures, liquid helium was drawn from the main reservoir through a needle valve. By a combination of adjusting the valve, with the automatically controlled power of the heater attached to a sample holder, the temperature was kept constant during scanning of the wavenumbers.

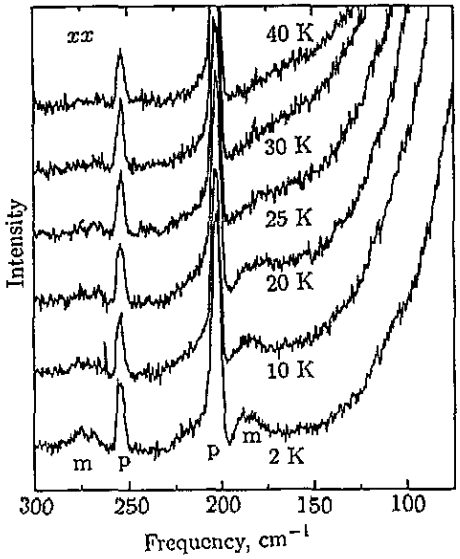

Figure 2. Raman spectra with the xx configuration of polarization of VCl_2, recorded at several temperatures. Phonon lines and magnetic lines are indicated as p and m, respectively.

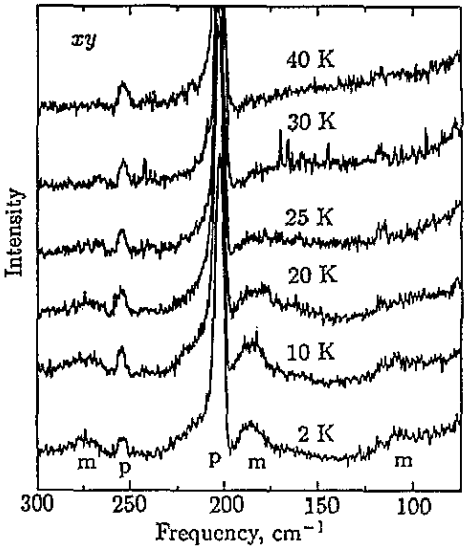

Figure 3. Raman spectra with the xy configuration of polarization of VCl_2, recorded at several temperatures. Phonon lines and magnetic lines are indicated as p and m, respectively.

We used a spectrometer, described in detail earlier [12], consisting of a double monochromator, a cooled photomultiplier and a photon counter, as well as several optical elements. The Raman spectra were excited with 514.5 nm radiation from an argon laser. To reduce self-heating of the sample, the power of the light was kept low for as long as the signal-to-noise ratio permitted. The best power was 50 mW. Owing to the lack of flat surfaces parallel to the c axis, it was impossible to employ a right-angle scattering geometry. Instead, we took the back-scattering spectra.

Because of the back-scattering geometry, where the incident and scattered light propagate along the z axis, the available configurations of the polarization of the incident and scattered light in the experiment were xx and xy. We show in figures 2 and 3 the Raman spectra observed over the temperature range $2 \sim 40$ K. The signal-to-noise ratio is bad, probably because of the unevenness of the sample surface. As indicated in these figures, we attribute the two lines denoted by 'p' to be phonon lines, and the three lines denoted by 'm' to be magnetic lines, based on the following

facts. The p lines are relatively sharp and strong in their intensities. They appear even at room temperature. The two p lines shift to the lower side monotonically with increasing temperature. The frequencies of both at room temprature decrease by $4\,cm^{-1}$ from those at 2 K.

The m lines, in contrast, are broad and weak. They become broader and weaker with increasing temperature, and they seem to disappear around $30 \sim 40$ K. It was impossible to trace them at higher temperatures. Due to the growing background over the lower-wavenumber region in the xx spectrum, we could not check whether the m line at $110\,cm^{-1}$ observed in the xy spectrum appears in the xx spectrum. These spectra are substantially similar to those reported in [10].

4. Discussion

4.1. Phonon lines

Since the phonon lines are similar to those observed and analyzed in several other CdI_2-type compounds [13], here we merely show the factor group analysis and confirm that the p lines certainly arise from phonon scattering. The unit cell has one molecule, i.e. one V atom and two Cl atoms, so nine normal modes are expected. Following the notation of the point group of D_{3d}, the irreducible representations are given by

$$A_{1g} + E_g + 2A_u + 2E_u .$$

Among these, both E_g and E_u are degenerate modes. The Raman-active modes are

$$A_{1g} + E_g$$

and their Raman tensors are

$$A_{1g} = \begin{pmatrix} a & & \\ & a & \\ & & b \end{pmatrix}$$

$$E_g = \begin{pmatrix} c & & \\ & -c & d \\ & d & \end{pmatrix} \qquad \begin{pmatrix} & -c & -d \\ -c & & \\ -d & & \end{pmatrix} .$$

The Stokes lines are then expected to be as follows: one line of the A_{1g} mode in xx, yy and zz; one line of the E_g mode in xx, yy, xy and xz. Because of the back-scattering geometry, only the xx $(= yy)$ and xy spectra were available in the present measurements. The A_{1g} mode should then appear only in the xx spectrum, and the E_g mode in both the xx and xy spectra. As can be seen in figures 2 and 3, the xx and xy spectra obtained at 2 K show two p lines at the same position at $202.5\,cm^{-1}$, whereas the other p line observed at 254.6 K is relatively stronger in the xx spectrum than in the xy spectrum. We found that the p line at $254.6\,cm^{-1}$ decreased in intensity when the polarization direction of the analyser for the scattering light was rotated from x to y, whereas the p line at $202.5\,cm^{-1}$ was independent of the rotation. This means that the p line appearing at $254.6\,cm^{-1}$ in the xy spectrum

is a leakage of the line appearing at the same position in the xx spectrum. Such a leakage is common in several compounds with a CdI_2 or $CdCl_2$ type of structure [14] and is recognized as being caused by an irregular alignment of the c axis within the crystals, which produces a residual depolarization.

As the harmonic oscillator model predicts [13], the A_{1g} mode and the E_g mode correspond to the vibration of the Cl atoms parallel and perpendicular to the c axis, respectively, and the A_{1g} mode has a higher frequency than the E_g mode. Thus we assign the p line at 254.6 cm^{-1} to the A_{1g} mode and that observed at 202.5 cm^{-1} to the E_g mode.

4.2. Magnetic lines

We now discuss the m lines. We first analyse them based on the assumption of magnon scattering, because neutron diffraction studies of this compound indicate a 120° structure in the ac plane. Because of the very weak anisotropy there is no possibility that the one-magnon line appears above 100 cm^{-1}; this will be discussed later. Thus we examine whether or not the observed m lines can be explained by two-magnon scattering.

We first develop spin-wave dispersion relations, assuming a 120° structure, and compare with experimental results. The Hamiltonian we treat is now given by

$$\mathcal{H} = 2J \sum_{i>j} \boldsymbol{S}_i \cdot \boldsymbol{S}_j + 2J' \sum_{l>m} \boldsymbol{S}_l \cdot \boldsymbol{S}_m \tag{1}$$

where the first and second terms are the intralayer and interlayer exchange interactions, respectively. Since the anisotropy is very small, we neglect it. With reference to the method developed by Oguchi [15], we obtain the dispersion relations reduced to the Γ–M zone to be

$$\begin{aligned} \hbar\omega_1 &= 2S\{[J(3-\Gamma_k(0)) + 2J'(1-\gamma_2)][J(3+2\Gamma_k(0)) + 4J'(1+\gamma_2)]\}^{1/2} \\ \hbar\omega_\pm &= 2S\{[J(3-\Gamma_k(\mp 2\pi/3)) + 2J'(1+\gamma_2)][J(3+2\Gamma_k(\mp 2\pi/3)) + 4J'(1-\gamma_2)]\}^{1/2} \end{aligned} \tag{2}$$

where

$$\gamma_{1k}(\theta) = \{\exp(-ik_x) + \exp[-i(-\tfrac{1}{2}k_x + \tfrac{\sqrt{3}}{2}k_y)] + \exp[-i(\tfrac{1}{2}k_x + \tfrac{\sqrt{3}}{2}k_y)]\}\exp(-i\theta)$$

and

$$\gamma_2 = \cos(2k_z) \qquad \Gamma_k(\theta) = \tfrac{1}{2}(\gamma_{1k}(\theta) + \gamma_{1k}^*(\theta)).$$

The dispersion relations given above substantially agree with the ones reported earlier [1, 2].

We next derive the spin-dependent electric polarizability following the method given by Moriya [16]. For the two-magnon process only the bilinear terms in the spin components are effective in α, and we therefore express it as

$$\alpha = \sum_{i>j} \alpha_{ij} \boldsymbol{S}_i \cdot \boldsymbol{S}_j. \tag{3}$$

The spin sites necessary to get α_{ij} are shown in figure 1. From a consideration of the local symmetry around a pair of V^{2+} ions, we obtain

$$\alpha_{01} = \alpha_{04} = \begin{pmatrix} a & & \\ & b & d \\ & d & c \end{pmatrix}$$

$$\alpha_{02} = \alpha_{05} = \frac{1}{4}\begin{pmatrix} a+3b & \sqrt{3}(b-a) & -2\sqrt{3}d \\ \sqrt{3}(b-a) & 3a+b & -2d \\ -2\sqrt{3}d & -2d & 4c \end{pmatrix} \tag{4}$$

$$\alpha_{03} = \alpha_{06} = \frac{1}{4}\begin{pmatrix} a+3b & \sqrt{3}(a-b) & 2\sqrt{3}d \\ \sqrt{3}(a-b) & 3a+b & -2d \\ 2\sqrt{3}d & -2d & 4c \end{pmatrix}.$$

As a result, the bilinear terms in α are expressed as

$$\begin{aligned}\alpha = \sum_{j=1}^{6} \alpha_{0j} S_0 \cdot S_j = {} & \frac{1}{2}\begin{pmatrix} p_1 & & \\ & p_1 & \\ & & p_2 \end{pmatrix} \sum_{j=1}^{6} \alpha_{0j} S_0 \cdot S_j \\ & + \frac{1}{2}\begin{pmatrix} -p_3 & & \\ & p_3 & p_4 \\ & p_4 & \end{pmatrix} [S_0 \cdot S_1 + S_0 \cdot S_4 - \tfrac{1}{2}(S_0 \cdot S_2 + S_0 \cdot S_3 + S_0 \cdot S_5 + S_0 \cdot S_6)] \\ & + \frac{\sqrt{3}}{2}\begin{pmatrix} & p_3 & -p_4 \\ p_3 & & \\ -p_4 & & \end{pmatrix} [S_0 \cdot S_2 + S_0 \cdot S_5 - (S_0 \cdot S_3 + S_0 \cdot S_6)]\end{aligned} \tag{5}$$

where

$$p_1 = a + b \qquad p_2 = 2c \qquad p_3 = b - a \qquad p_4 = 2d.$$

The electric dipole moment, $P(t)$, induced by the incident light with a frequency ω_0 of the electric field, is given in the long-wave approximation by

$$P(t) = \exp(i\mathcal{H}t/\hbar)\,\alpha\,\exp(-i\mathcal{H}t/\hbar)\,E_0\,\exp(-i\omega_0 t). \tag{6}$$

Since the first term in equation (5) is commutable with $\mathcal{H}$, no spin-fluctuation effect on $P(t)$ arises, whereas the second and third terms do not commute with $\mathcal{H}$. These two terms therefore bring about the two-magnon scattering. To see the dependence of α on the wavevector in the first Brillouin zone, we make a Fourier transform of S_i. We then obtain the final expression of α to be

$$\alpha = \sum_k S_k \cdot S_{-k}\left[\begin{pmatrix} -p_3 & & \\ & p_3 & p_4 \\ & p_4 & \end{pmatrix}\Gamma_1 + \begin{pmatrix} & p_3 & -p_4 \\ p_3 & & \\ -p_4 & & \end{pmatrix}\Gamma_2\right] \tag{7}$$

where

$$\begin{aligned}\Gamma_1 &= 2\cos k_x - \cos(\tfrac{1}{2}k_x + \tfrac{\sqrt{3}}{2}k_y) - \cos(-\tfrac{1}{2}k_x + \tfrac{\sqrt{3}}{2}k_y) \\ \Gamma_2 &= \sqrt{3}[\cos(\tfrac{1}{2}k_x + \tfrac{\sqrt{3}}{2}k_y) - \cos(-\tfrac{1}{2}k_x + \tfrac{\sqrt{3}}{2}k_y)].\end{aligned} \tag{8}$$

Both Γ_1 and Γ_2 have their maximum values at the symmetry point M and its equivalents in the first Brillouin zone, as shown in figure 4.

As the light-scattering theory indicates, the scattering intensity is approximately proportional to α^2. Since this value is extremely large at the symmetry point M, it is these magnons that play a dominant role in two-magnon scattering. Moreover, the matrices in equation (7) show the configurations of polarization of the incident and scattered light that can produce two-magnon scattering. That is, we easily find that the $xx(=yy)$, xy and xz spectra will show the two-magnon lines.

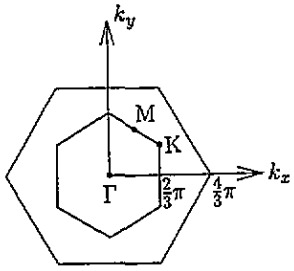

Figure 4. First Brillouin zone. The inner and outer zones correspond to the magnetic and crystallographic ones, respectively.

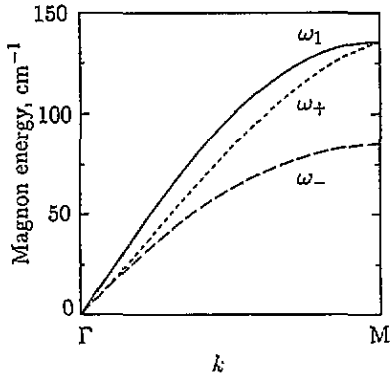

Figure 5. Dispersion relations calculated using the values of $S = \frac{3}{2}$, $J = 22\,\mathrm{K}$ and $J' = 0.135\,\mathrm{K}$.

We now return to the experimental results, and compare them with the theory developed above. When the values $J = 22\,\mathrm{K}$ and $J' = 0.135\,\mathrm{K}$, determined from neutron diffraction measurements [1,2], and $S = \frac{3}{2}$ are introduced in equation (2), we obtain the dispersion curves of the three modes ω_1, ω_+ and ω_-, which are shown in figure 5. The values at the zone edge are $\omega_1^{ze} = 146.7\,\mathrm{cm}^{-1}$, $\omega_+^{ze} = 145.8\,\mathrm{cm}^{-1}$ and $\omega_-^{ze} = 92.0\,\mathrm{cm}^{-1}$. The two modes ω_1 and ω_+ are practically degenerate at the M point. We find that the frequencies of the two m lines, i.e. $247\,\mathrm{cm}^{-1}$ and $186\,\mathrm{cm}^{-1}$, are nearly equal to the values of $2\omega_1^{ze} \simeq 2\omega_+^{ze} \simeq 292\,\mathrm{cm}^{-1}$ and $2\omega_-^{ze} \simeq 184\,\mathrm{cm}^{-1}$, respectively. We therefore reasonably conclude that the observed m lines at $247\,\mathrm{cm}^{-1}$ and $186\,\mathrm{cm}^{-1}$ are due to scattering from pairs of zone-edge magnons having the frequencies given above.

A question arises, however, when we remember that the two-magnon processes persist in the Raman scattering intensity far above T_N [17]. The two present m lines attributed to two-magnon processes seem to disappear above $T_N = 36\,K$, which is close to $T_{KM} = 33\,K$ calculated using the formula given by KM. This unusual decrease in intensity suggests, in our opinion, a possible effect of the Z_2 vortex. That is, spontaneous generation of the vortices above $T_N \approx T_{KM}$ should influence the fluctuation of spins having the zone-edge wavenumber. Consequently, the intensity of the two-magnon lines can have a temperature dependence different from that observed in conventional antiferromagnets. Further theoretical investigations of this suggestion are anticipated.

The m line appearing at $110\,cm^{-1}$, however, is impossible to attribute to two-magnon scattering. As already briefly mentioned, the one-magnon line, if it appears, should be at a frequency lower than $1\,cm^{-1}$ because the energies of the magnons at the zone centre less than $1\,cm^{-1}$ owing to the small anisotropy. Moreover, the one-magnon line should have a very low intensity, not enough to be observable, because the intensity is proportional to $(H_A/2H_E)^{1/2}$ where H_A and H_E are the anisotropy field and the exchange field, respectively [17]. This means that Heisenberg magnets such as VCl_2, which has $H_A/H_E \sim 10^{-4}$, cannot yield one-magnon scattering lines having an intensity strong enough to be observable. The effect of the electron–phonon coupling mechanism, introduced in [10], is absolutely ruled out in the present case because the symmetry of the 120° structure results in $\sum r_{ij} S_i \cdot S_j = 0$.

At present we cannot explain the origin of the m line at $110\,cm^{-1}$. Does the inherent frustration, or some hidden disorder expected in VCl_2, produce extra magnetic Raman lines? We have no answer to this question. As the neutron diffraction [1, 2] and EPR studies [9] revealed, the effect of the Z_2 vortex appears in the paramagnetic region near T_N. Unfortunately, our present data give no information near T_N because the intensity of the three m lines is very weak and is under noise near and above T_N.

In conclusion, we detected three magnetic Raman scattering lines in VCl_2 at low temperature. Two of them are successfully attributed to the two magnon lines of the 120° structure, but the other line remains unsolved. We hope for theoretical developments concerning the influence of the generation of Z_2 vortices on the scattering intensity of two-magnon processes. (Using the same point of view as in the present case, a Raman scattering investigation has been made on another triangular-lattice Heisenberg antiferromagnet, $LiCrO_2$ [18]; we expect the results will be published later in *J. Phys.: Condens. Matter*.)

Acknowledgments

We are grateful to Professor K Hirakawa for supplying us with single crystals of VCl_2. Thanks are due to Mr M Suzuki for technical assistance.

References

[1] Kadowaki H, Ubukoshi K and Hirakawa K 1985 *J. Phys. Soc. Japan* **54** 363 and references therein

[2] Kadowaki H, Ubukoshi K, Hirakawa K, Martínez J L and Shirane G 1987 *J. Phys. Soc. Japan* **56** 4027 and references therein. The results of the studies on VCl_2 and VBr_2 are reviewed compactly in

de Jongh L J (ed) 1990 *Magnetic Properties of Layered Transition Metal Compounds* (Dordrecht: Kluwer) p 259

[3] Anderson P W 1973 *Mat. Res. Bull.* **8** 153
[4] Hirakawa K, Ikeda H, Kadowaki H and Ubukoshi K 1983 *J. Phys. Soc. Japan* **52** 2882
[5] Yamada I, Ubukoshi K and Hirakawa K 1984 *J. Phys. Soc. Japan* **53** 381
[6] Takeda K, Ubukoshi K, Haseda T and Hirakawa K 1984 *J. Phys. Soc. Japan* **53** 1480
[7] Niel M, Cros C, Le Flem G, Pouchard M and Hagenmuller P 1977 *Physica* B **86–88** 702
[8] Kawamura H and Miyashita S 1984 *J. Phys. Soc. Japan* **53** 4318
[9] Ajiro Y, Kikuchi H, Sugiyama S, Nakashima T, Shamoto S, Nakayama N, Kiyama M, Yamamoto N and Oka Y 1988 *J. Phys. Soc. Japan* **57** 2268
[10] Bauhofer W, Güntherodt G, Anastassakis E, Frey A and Benedek G 1980 *Phys. Rev.* B **22** 5873
[11] Kuindersma S R, Haas C, Sanchez J P and Al R 1979 *Solid State Commun.* **30** 403
[12] Totani M, Fukada Y and Yamada I 1989 *Phys. Rev.* B **40** 10577
[13] Frey A and Benedek G 1979 *Solid State Commun.* **32** 305
[14] Lockwood D J 1973 *J. Opt. Soc. Am.* **63** 374
[15] Oguchi T 1983 *J. Phys. Soc. Japan* **52** 183 (suppl)
[16] Moriya T 1967 *J. Phys. Soc. Japan* **23** 490
[17] Fleury P A and Loudon R 1968 *Phys. Rev.* **166** 514
[18] Suzuki M, Yamada I, Kadowaki H and Takei F 1993 *J. Phys.: Condens. Matter* to be submitted